



## NUMERICAL STUDY ON THE STABILITY OF ELASTOMERIC SEISMIC ISOLATION BEARINGS

Gordon P. Warn<sup>1</sup> and Jared R. Weisman<sup>2</sup>

### ABSTRACT

An important consideration for the design of seismic isolation systems composed of elastomeric bearings is the safety of individual bearings for maximum considered earthquake shaking. One assessment of bearing safety requires the bearing be stable at the maximum displacement that requires the reduced critical load carrying capacity be greater than the compressive load imposed on the bearing. Typically the reduced critical load carrying capacity is assessed using an overlapping area procedure whereby the critical load capacity at zero lateral displacement is reduced by the ratio of the overlapping area between the top and bottom bearing end plates divided by the total bonded rubber area for a given lateral displacement. Although the overlapping area procedure provides a simple method of estimating the load carrying capacity of an elastomeric seismic isolation bearing in the laterally deformed configuration previous research suggest the predictions are overly conservative and do not agree well with experimental data. This paper presents the results of a numerical study of the stability of an elastomeric seismic isolation bearing under large lateral displacement using the finite element method (FE). Results from the FE analyses show that the reduction in critical load carrying capacity does not decrease linearly with increasing lateral displacement as is approximately suggested by the overlapping area approach. A comparison of the FE results with the reduced critical load predicted by the overlapping area procedure suggests that the overlapping area approach significantly underestimates the load carrying capacity of elastomeric bearings in the laterally deformed configuration predicting zero capacity at a lateral displacement equal to the bearing diameter. An improved formula for predicting the reduction in critical load with lateral displacement based on the Koh-Kelly two-spring model is explored.

---

<sup>1</sup>Assistant Professor, Dept. of Civil Engineering, The Pennsylvania State University, University Park, PA 16802

<sup>2</sup>Graduate Research Assistant, Dept. of Civil Engineering, The Pennsylvania State University, University Park, PA 16802

## Introduction

Seismic isolation is a method of protecting a structure and its components from the damaging effects of earthquake ground motion by shifting the period of the isolated structure away from the predominant frequency content of the ground motion. This period shift is achieved through horizontally flexible isolators used to decouple the superstructure from the supporting substructure. Under moderate to large earthquake ground shaking, the increased period of the isolated structures typically translates into large lateral displacements across the isolation interface possibly accompanied by large axial compressive loads from overturning forces on some individual isolators. Elastomeric bearings are one type of isolator consisting of a number of alternating elastomeric (rubber) layers bonded to intermediate steel (shim) plates. The horizontal flexibility (shear stiffness) of an elastomeric bearing is dictated by the total thickness of rubber whereas the close spacing of the intermediate shim plates provides a large vertical (relative to the shear) stiffness for a given shear modulus and bonded rubber diameter. An important consideration for design is the stability of the individual elastomeric bearings under large lateral displacement and simultaneous axial compressive loading. It has been shown that these large lateral displacements might lead to substantial reductions in the load-carrying capacity of elastomeric bearings (Buckle and Liu 1994; Nagarajaiah and Ferrell 1999; and Buckle et al. 2002) and yet there is currently no codified procedure for assessing the stability in the laterally deformed configuration. One commonly used method for this assessment, although not codified, was introduced by Buckle and Liu (1994) that uses the ratio of overlapping area between the bearing top and bottom plates to the bonded rubber area at a given lateral displacement to reduce the critical load carrying capacity of elastomeric bearings in the undeformed configuration ( $P_{cr}$ ). Figure 1 illustrates the overlapping area for a laterally deformed circular bearing. The reduced critical load carrying capacity ( $P'_{cr}$ ) for a given lateral displacement ( $u$ ) is calculated according to:

$$P'_{cr} = \left( \frac{A_r}{A_b} \right) \cdot P_{cr} \quad (1)$$

where  $A_b$  is the bonded rubber area;  $A_r$  is the overlapping area between the bearing end plates and  $P_{cr}$  is the critical load of the elastomeric bearing in the undeformed configuration (Kelly 1997) calculated using:

$$P_{cr} = \sqrt{(GA_s)_{eff} P_E} \quad (2)$$

where  $(GA_s)_{eff}$  is the effective shear rigidity of the bearing;  $G$  is the shear modulus of the elastomer;  $A_s$  is the effective shear area; and  $P_E$  is the Euler buckling load of the bearing. Details on the calculation of  $P_{cr}$  for elastomeric bearings can be found in Kelly (1997).

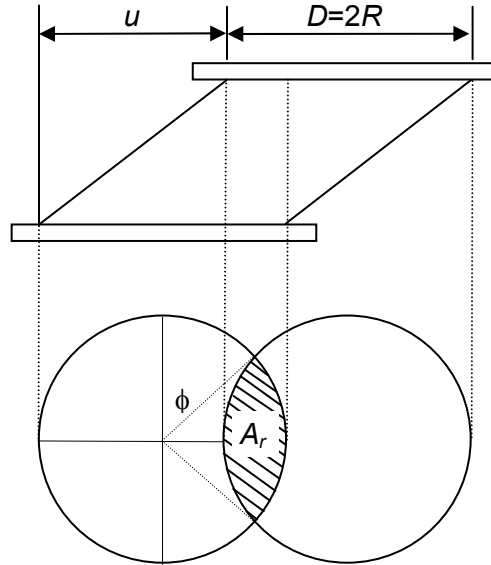


Figure 1. Illustration of overlapping area

Although the overlapping area procedure provides a convenient method for assessing the stability of elastomeric bearing in the laterally deformed configuration the approach predicts zero load carrying capacity at a lateral displacement equal to the bearing diameter while experimental evidence has suggested that the reduced load carrying capacity at this level of displacement could range from 20% to 50% of  $P_{cr}$  for square bearings with shape factors from 1.67 to 5 (Nagarajaiah and Ferrell 1999; and Buckle et al. 2002). The shape factor ( $S$ ) is defined as the ratio of the loaded area divided by the area free to bulge for an individual rubber layer. These results, although limited to square bearings with low shape factors (low for seismic isolation applications) suggest the overlapping area method: (i) does not capture well the stability behavior of the elastomeric bearing in the laterally deformed configuration and (ii) might provide overly conservative estimates of the load carrying capacity of elastomeric bearings in the laterally deformed configurations.

### Objectives

The objectives of this study are: (i) to investigate the stability of an elastomeric seismic isolation bearing (having a shape factor  $> 5$ ) in the laterally deformed configuration using detailed nonlinear finite element (FE) analysis; (ii) to evaluate the reduced load carrying capacity predicted by the overlapping area procedure using the results of the FE study; and (iii) to explore an improved analytical formulation for predicting the reduced load carrying capacity based on a two-spring mechanical model (Koh and Kelly 1987) using numerical sensitivity analysis. The general purpose finite element software package ABAQUS (DSSC 2008) was used to model and investigate the stability of a scaled low-damping rubber bearing utilized for earthquake simulation testing (Warn and Whittaker 2008). The stability of the low-damping rubber bearing is studied using the results of a series of FE analyses that subjected the bearing to simultaneous axial compressive load and lateral displacement for a range of compressive load levels. The development of an improved analytical formulation based on a two-spring mechanical model introduced by Koh and Kelly (1987) for predicting the reduced load carrying capacity of elastomeric bearings is explored by numerically investigating the sensitivity of the two-spring

solution to various material (i.e., spring) and geometric assumptions. Results of the sensitivity analyses are intended to provide guidance as to the level of assumptions necessary for a robust analytical formulation.

### Finite Element Study of an Elastomeric Seismic Isolation Bearing

#### Model Description

A three-dimensional half-space FE model of a low-damping rubber bearing with shape factor,  $S$ , equal to 10 utilized for earthquake simulation testing (Warn and Whittaker 2008) was developed in ABAQUS Version 6.8-1. The bearing is annular with an outer diameter of 152 mm, an inner diameter of 30 mm, 20 rubber layers each 3 mm thick providing a total thickness of rubber of 60 m and two 25 mm thick internal end-plates. A detailed cross-section of the low-damping rubber bearing is presented in Fig. 2a. Figure 2b presents an illustration of the FE model in the deformed configuration.

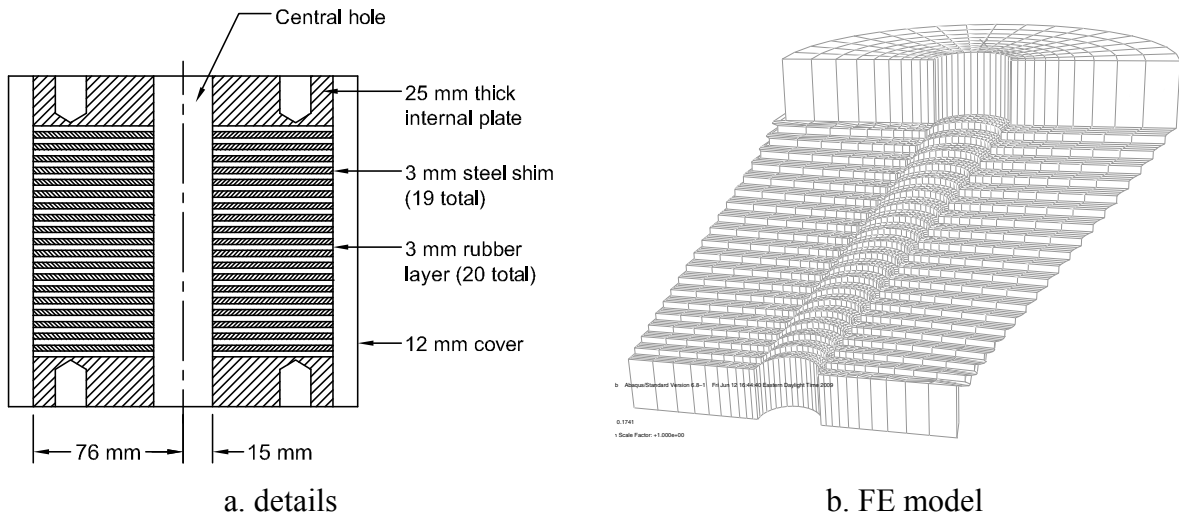


Figure 2. Elastomeric seismic isolation bearing

#### Material Properties

The steel shim plates and bearing end-plates were modeled with linear elastic material properties assuming a Young's modulus of 200  $GPa$  and a Poisson's ratio of 0.3.

The Neo-Hookean model was chosen for the rubber material because of the direct relationship between the material constants and engineering properties of the rubber. The model assumes the rubber to be linear, isotropic and incompressible or nearly incompressible. The constitutive behavior of the hyperelastic material model is defined by the strain energy potential,  $W$ , that for the Neo-Hookean material model is:

$$W = C_{10} (\bar{I}_1 - 3) + \frac{1}{D_1} (J^{el} - 1)^2 \quad (3)$$

where  $C_{10}$  and  $D_1$  are material parameters,  $\bar{I}_1$  is the first stress invariant and  $J^{el}$  is the elastic volume ratio. The shear modulus,  $G$ , and bulk modulus,  $K$ , are related to the material parameters according to:

$$G = 2C_{10} \quad (4)$$

$$K = \frac{2}{D_1} \quad (5)$$

Table 1 presents values of the material parameter and corresponding shear and bulk moduli. The rubber was modeled as nearly incompressible with an assumed bulk modulus of 2000 MPa and a shear modulus of 0.68 MPa corresponding to the effective shear modulus at 100 percent shear strain determined from characterization testing performed on an identical low damping rubber bearing (Warn and Whittaker 2008).

Table 1. Material parameters for the Neo-Hookean model.

Material Model	$C_{10}$ MPa	$C_{01}$ MPa	$D_1$ 1/MPa	$G$ MPa	$K$ MPa
Neo-Hookean	0.34	0	0.00099	0.68	2000

### Boundary Conditions and Loading

For the stability analysis the bottom bearing end-plate was restrained against rotation and translation. The top bearing end-plate was allowed to translate in the vertical and lateral directions but restrained against rotation. To prevent torsion the vertical load and lateral displacement were applied through the centroid of the bearing top-plate. An additional restraint was applied to the intermediate rubber layers to prevent bulging in the out-of-plane direction on the cut surface that would be restrained by the other half of the bearing.

### Numerical Results of Stability Analysis

The stability limit of the elastomeric bearing in the laterally deformed configuration is identified as the point at which the shear force passes through a maximum value (Nagarajaiah and Ferrell 1999) corresponding to the point where the tangential horizontal stiffness equal zero for a given axial compressive load. Stability data was obtained by performing a series of static, nonlinear, FE analyses whereby the bearing model was subjected to combined axial compressive load and sheared through a lateral displacement. Two analysis procedures were used. For low axial compressive load levels, the FE analyses were performed by first subjecting the bearing to a constant axial compressive load then shearing it to a target lateral displacement. However, for high axial compressive loads (greater than 60% of  $P_{cr}$ ) the FE analysis failed to reach a significant lateral displacement. Therefore for axial compressive load greater than 67 kN, a second analysis procedure was used that subjecting the FE model to simultaneously increasing axial compressive load and lateral displacement to a specified displacement less than the target displacement. The analysis then continued by shearing the bearing under the constant axial compressive load to the target displacement. This procedure was performed for the axial load level of 67 kN to verify the stability point was not affected by the analysis procedure. The values of the axial compressive load and lateral displacement where the tangential horizontal stiffness equaled zero were identified as the reduced critical load ( $P'_{cr}$ ) and critical displacement ( $u_{cr}$ ).

Figure 4 presents sample force-displacement curves from the FE model for axial compressive loads ranging from zero to 222 kN (equivalent to 12.7 MPa of vertical compressive

pressure). The results presented in Fig. 4 show that as the axial compressive load increases the shear force passes through a maximum value and that the displacement at which the maximum value occurs decreases with increasing axial load. This result has been observed by others (Buckle and Liu 1994; and Buckle et al. 2002) from experimental testing and 2-D finite element analysis of square laminated rubber bearing. A discontinuity in the force-displacement curves for axial loads greater than 67 kN is a result of the second analysis procedure.

The reduced critical load ( $P'_{cr}$ ) results obtained from the FE analyses were normalized by the critical load ( $P_{cr}$ ) of the bearing calculated to be 290 kN using to Eq. 2. Normalized reduced critical load ( $P'_{cr}/P_{cr}$ ) data plotted as a function of the corresponding critical displacement ( $u_{cr}$ ) normalized by the bearing diameter ( $D$ ) is plotted in Fig. 5. Also plotted in Fig. 5, is the reduced critical load predicted by the overlapping area procedure also in normalized format. The FE results presented in Fig. 5, show the normalized reduced critical load decreases with increasing lateral displacement having a value of 0.28 at a  $u/D$  approximately equal to 1. Comparison of the FE stability data with that predicted by the overlapping area procedure suggests the overlapping area procedure significantly underestimates the load carrying capacity for all lateral displacements notably predicting zero load carrying capacity at a lateral displacement equal to the bearing diameter whereas the detailed FE analysis suggest approximately 28% of the loading carrying capacity remains. Further, this comparison shows the overlapping area procedure does not capture well the observed behavior of the elastomeric bearing.

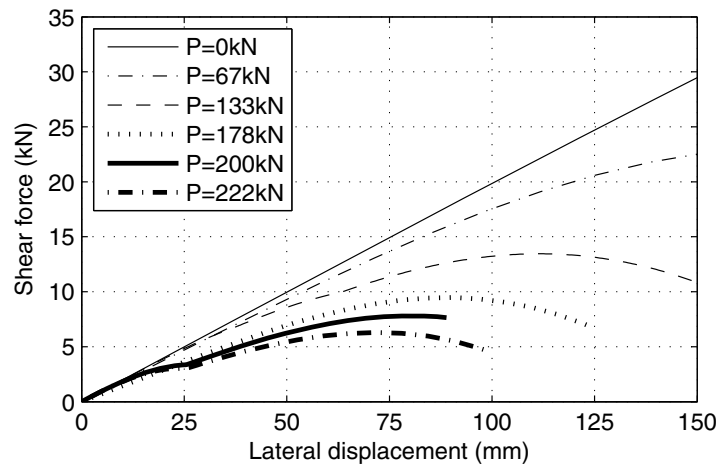


Figure 4. Force-displacement response of bearing for varying axial load levels

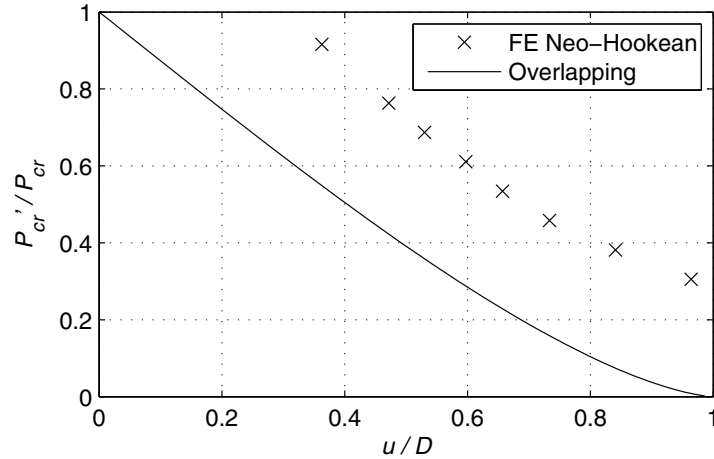


Figure 5. Stability results from FE analysis

### Numerical Analysis of the Two-Spring Model

The results presented in Fig. 5 motivated an exploration for an improved method of predicting the reduced critical load carrying capacity of elastomeric bearings at a given lateral displacement. A two-spring mechanical representation of an elastomeric bearing introduced by Koh and Kelly (1987) was first considered for the derivation of an improved formula. The two-spring model has been shown to capture the coupled horizontal and vertical behavior of elastomeric bearings well predicting the reduction in horizontal stiffness and damping with increasing axial load (Kelly 1997). In addition the two-spring model was shown to predict with reasonable accuracy the reduction in vertical stiffness with lateral displacement observed from experimental testing of low-damping rubber and lead-rubber bearings (Warn et al. 2007). The application of the two-spring model to predict the stability of square elastomeric bearings was explored (Nagarajaiah and Ferrell 1999) showing the two-spring model might be capable of providing improved estimates of the reduced critical load carrying capacity however a closed-form formula was not pursued. This section presents the results of a sensitivity analysis of the two-spring solution to various material and geometric assumptions. Results of the sensitivity analysis are being used to guide the development of a closed-form solution for the reduced critical load carrying capacity derived from the two-spring model. Derivation of the closed-form is ongoing therefore the final form could not be presented in this paper.

### Two-Spring Model

Figure 6 presents an illustration of the two-spring model in the undeformed (Fig. 6a) and laterally deformed (Fig. 6b) configurations. The model consists of a linear spring with stiffness,  $K_s$ , a rotational spring with stiffness,  $K_\theta$ , two frictionless rollers, and a rigid tee supported by a pin with total height,  $h$ . Also shown in Fig. 6 are the applied loads,  $P$  and  $F$ , and the resulting deformations, namely, the lateral displacement at the top of the column,  $u$ , rotation about the pin,  $\theta$ , reduction in height,  $\delta_v$ , and deformation of the linear spring,  $s$ . Relating the spring properties of the model to the mechanical properties of an elastomeric seismic isolation bearing provides a simple physical understanding of the behavior under combined lateral and vertical loading (Kelly 1997).

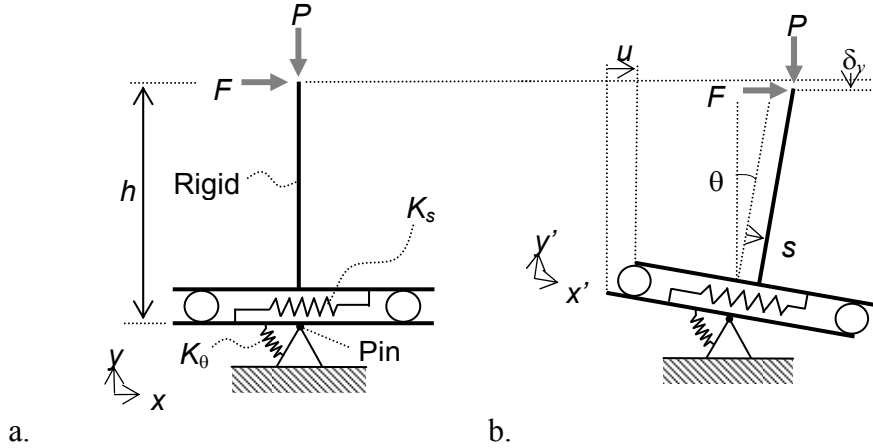


Figure 6. Illustration of two-spring model: (a) undeformed and (b) deformed configuration

Considering the model in the deformed configuration the following equilibrium equations are obtained:

$$K_s \cdot s = F \cdot \cos(\theta) + P \cdot \sin(\theta) \quad (6)$$

$$K_\theta \cdot \theta = P \cdot [h \cdot \sin(\theta) + s \cdot \cos(\theta)] + F \cdot [h \cdot \cos(\theta) - s \cdot \sin(\theta)] \quad (7)$$

Further, compatibility of the model requires the lateral displacement,  $u$ , is related to the local deformations quantities  $s$  and  $\theta$ , according to:

$$u = h \cdot \sin(\theta) + s \cdot \cos(\theta) \quad (8)$$

Equations (6) and (7) were solved numerically with different material (spring) and geometric assumptions to determine the sensitivity of the equilibrium solution and to identify the key material and geometric assumptions necessary for the two-spring model to capture the instability behavior of elastomeric bearings.

### Sensitivity of Two-Spring Solution

The sensitivity of the two-spring solution to different material (spring) and geometric assumptions was studied to determine the level of complexity necessary for the two-spring model to predict the reduction in load carrying capacity with increasing lateral displacement. Five cases were considered: (1) linear springs – linear geometry; (2) linear springs – nonlinear geometry; (3) nonlinear  $K_s$  - nonlinear geometry; (4) nonlinear  $K_\theta$  - nonlinear geometry; and (5) nonlinear springs – nonlinear geometry.

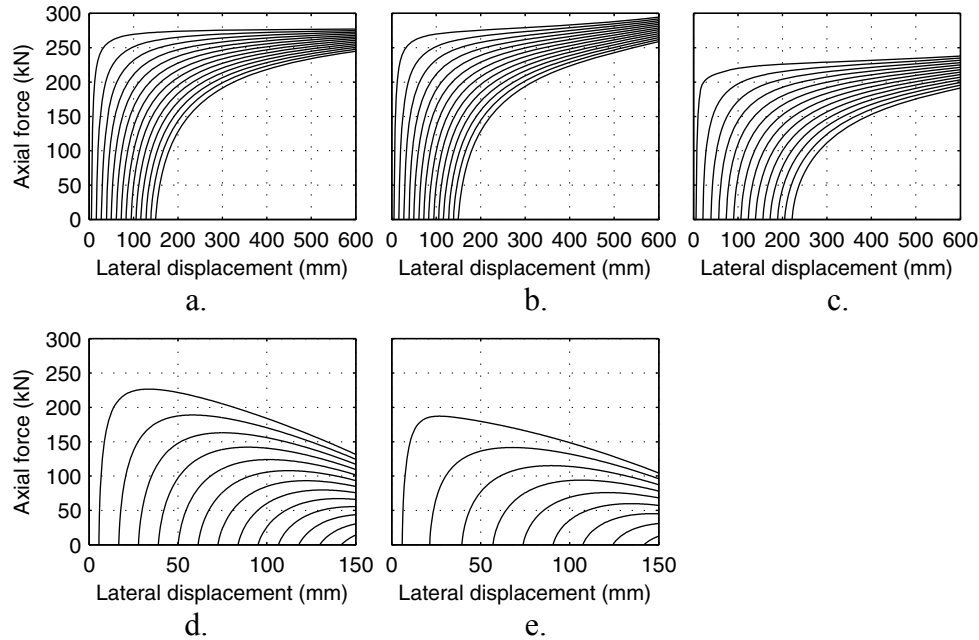


Figure 7. Sensitivity of the two-spring solution to the following assumptions: (a) Linear; (b) Linear springs-nonlinear geometry; (c) nonlinear  $K_s$  and geometry ; (d) nonlinear  $K_\theta$  and nonlinear geometry and (e) nonlinear springs and nonlinear geometry.

The solution of the equilibrium equations for the five cases was obtained using a numerical routine to solve simultaneous nonlinear equations in Matlab (Mathworks 2008). For cases with linear spring properties, the constants  $K_s$  and  $K_\theta$  were assigned values based on the calculated shear stiffness and rotational stiffness of the low-damping rubber bearing using the same geometric and material properties used for the FE analysis. For cases with linear geometry the  $\sin(\theta)$  and  $\cos(\theta)$  terms were replaced with  $\theta$  and 1, respectively. For cases with nonlinear spring properties  $K_s$  and  $K_\theta$  were assumed to reduce with shear displacement,  $s$  and rotation  $\theta$  using relationships proposed by Nagarajaiah and Ferrell (1999). Numerical solutions for the equilibrium of the two-spring model for the five cases are presented in Fig. 7 in the form of axial force versus lateral displacement curves. Each curve in Fig. 7 represents a constant shear force value. The results presented in Fig. 7 suggest that the nonlinearity in the rotational spring ( $K_\theta$ ) must be considered along with nonlinear geometry for the two-spring model to predict a reduction in load carrying capacity with increasing lateral displacement.

## Results

Fig. 8 presents a comparison of the predicted stability of the low-damping rubber bearing from the FE model, the two-spring numerical solution and the overlapping area procedure. As shown before the overlapping area procedure underestimates the stability of the elastomeric bearing by comparison to the FE results. The two-spring stability curve does predict load carrying capacity at a displacement equal to the bearing diameter ( $u/D = 1$ ) however the trend of the curve differs substantially from the FE results. Preliminary results, although not presented, here suggest the two-spring stability curve is sensitivity to the form of the nonlinear relationship between the spring properties and displacement quantities.

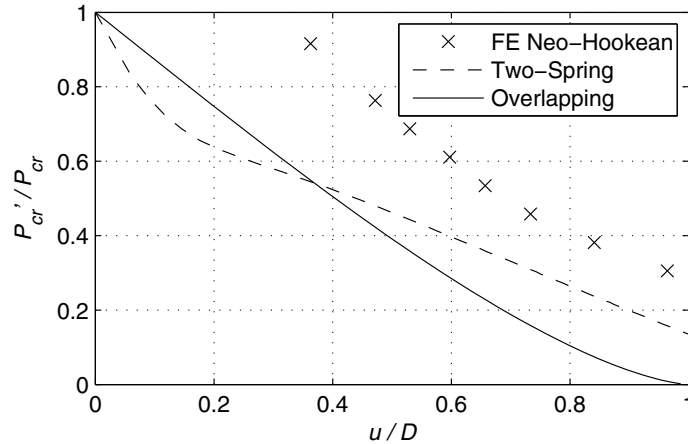


Figure 8. Comparison of predicted stability for low-damping rubber bearing

### Conclusions

This paper presented preliminary results of a numerical study on the stability of an elastomeric seismic isolation bearing. Although the results of this study are preliminary the following conclusions are suggested: (i) based on the FE investigation the stability or load carrying capacity of an elastomeric seismic isolation bearing with shape factor of 10 reduces with increasing lateral displacement to approximately 30% of the critical load at a lateral displacement equal to the bearing diameter (250% shear strain); (ii) the predicted stability using the overlapping area procedure significantly underestimates the load carrying capacity by comparison to the FE analysis and does not capture well the behavior of the elastomeric bearing in the laterally deformed configuration; and (iii) the two-spring model might be a viable alternative for the development of an improved analytical formulation for the predicting stability of elastomeric bearings however an improved understanding of the nonlinear spring properties is needed.

### References

- Buckle, I.G. and H. Liu, (1994). Experimental Determination of Critical Loads of Elastomeric Isolators at High Shear Strain, *NCEER Bulletin*, Vol 8, No 3, 1-5.
- Buckle, I.G., S. Nagarajaiah, and K. Ferrell, (2002). Stability of Elastomeric Isolation Bearings: Experimental Study, *ASCE Journal of Structural Engineering*, Vol 128, No. 1, 3-11.
- DSSC (2008). *ABAQUS/CAE User's Manual: Version 6.8-1*. Dassault Systèmes Simulia Corp., Providence, RI.
- Kelly, J.M., (1997). *Earthquake Resistant Design with Rubber*, 2<sup>nd</sup> Ed. Springer Verlag, NY.
- Koh, C.G. and J.M. Kelly, (1987). Effects of Axial Load on Elastomeric Bearings, UCB/EERC – 86/12, Earthquake Engineering Research Center, University of California, Berkeley.
- MathWorks, (2008). *MATLAB Version 7.6.0.324*. The MathWorks, Inc., Natick, MA.
- Nagarajaiah, S. and K. Ferrell, (1999). Stability of Elastomeric Isolation Bearings, *ASCE Journal of Structural Engineering*, Vol. 125, No. 9, 946-954.
- Warn, G.P., A.S. Whittaker, and M.C. Constantinou, (2007). Vertical Stiffness of Elastomeric and Lead-Rubber Seismic Isolation Bearings, *ASCE Journal of Structural Engineering*, Vol. 133, No. 9, 1227-1236.
- Warn, G.P. and A.S. Whittaker, (2008). Vertical Earthquake Loads on Seismic Isolation Systems in Bridges, *ASCE Journal of Structural Engineering*, Vol. 134, No. 11, 1696-1704.